

A region segmentation based algorithm for building a crystal position lookup table in a scintillation detector^{*}

WANG Hai-Peng(王海鹏)^{1,2,3} YUN Ming-Kai(贡明凯)^{1,2} LIU Shuang-Quan(刘双全)^{1,2} FAN Xin(樊馨)^{1,2,3}
CAO Xue-Xiang(曹学香)^{1,2} CHAI Pei(柴培)^{1,2} SHAN Bao-Ci(单保慈)^{1,2;1)}

¹ Key Laboratory of Nuclear Radiation and Nuclear Energy Technology, Institute of High Energy Physics, Chinese Academy of Sciences, Beijing 100049, China

² Beijing Engineering Research Center of Radiographic Techniques and Equipment, Beijing 100049, China

³ University of Chinese Academy of Sciences, Beijing 100049, China

Abstract: In a scintillation detector, scintillation crystals are typically made into a 2-dimensional modular array. The location of incident gamma-ray needs be calibrated due to spatial response nonlinearity. Generally, position histograms—the characteristic flood response of scintillation detectors—are used for position calibration. In this paper, a position calibration method based on a crystal position lookup table which maps the inaccurate location calculated by Anger logic to the exact hitting crystal position has been proposed. Firstly, the position histogram is preprocessed, such as noise reduction and image enhancement. Then the processed position histogram is segmented into disconnected regions, and crystal marking points are labeled by finding the centroids of regions. Finally, crystal boundaries are determined and the crystal position lookup table is generated. The scheme is evaluated by the whole-body positron emission tomography (PET) scanner and breast dedicated single photon emission computed tomography scanner developed by the Institute of High Energy Physics, Chinese Academy of Sciences. The results demonstrate that the algorithm is accurate, efficient, robust and applicable to any configurations of scintillation detector.

Key words: position lookup table, position histogram, region segmentation, scintillation detector

PACS: 07.85.-m, 07.85.Fv **DOI:** 10.1088/1674-1137/39/3/038201

1 Introduction

Scintillation detectors have been widely applied in nuclear medical imaging systems such as the positron emission tomography (PET) scanner and the single photon emission computed tomography scanner to detect the position, energy and time information of gamma-rays. A scintillation detector module consists of a 2-dimensional array of crystals coupled with photomultiplier tubes (PMTs) or position sensitive photomultiplier tubes (PSPMTs) [1]. These crystals are arranged in a matrix and separated by opaque material to prevent scintillation photons from traversing between crystals. When a scintillation crystal undergoes gamma-ray interaction, scintillation photons are generated. Then the photons are collected and converted to electronic signals by the PMTs or PSPMTs [2]. Using the signals and Anger positioning algorithm [3], the position coordinate (x, y) can be calculated to be the gamma-ray incidence position. However, because of spatial response nonlinearity

in the detection system, the calculated position coordinate cannot reflect the gamma-ray incidence position directly. The location inaccuracy will impair the spatial resolution of the detector seriously [4]. So position calibration needs to be done to correct the mistaken location. Generally, a crystal position lookup table, mapping the calculated position coordinates to incident crystal indexes is used for position calibration [5]. In order to build the crystal position lookup table, a flood image, which is the histogram of detected gamma-ray counts in each calculated position coordinate, is employed. An array of spots are shown in the position histogram. Each spot corresponds to a single crystal in the crystals array. So a crystal position lookup table can be built by segmenting the spot regions and labelling each region with the corresponding crystal index.

At present, several approaches have been proposed to build the crystal position lookup table using a position histogram. A maximum likelihood estimation method based on Gaussian mixture models (GMMs) was present-

Received 4 May 2014, Revised 12 June 2014

^{*} Supported by National Natural Science Foundation of China (81101175) and XIE Jia-Lin Foundation of Institute of High Energy Physics (Y3546360U2)

1) E-mail: shanbc@ihep.ac.cn

©2015 Chinese Physical Society and the Institute of High Energy Physics of the Chinese Academy of Sciences and the Institute of Modern Physics of the Chinese Academy of Sciences and IOP Publishing Ltd

ed by Stonger et al. [6]. The approach decreases the probability of mistaken crystal identification, and is suitable for any possible crystal configuration. However, that is impractical for the large dimension position histogram, because a large number of parameters for the GMMs must be estimated. An approach to determining valley points as crystal boundary points in a position histogram was proposed by Chai et al. [7], which was also based on GMMs. This method is efficient in the case of small crystal arrays with uniform characteristics, but it is time-consuming to correct the crystal marking points interactively when the crystal number is large or the response of crystals varies dramatically. An approach based on neural networks and self-organizing feature maps was implemented by Lazzerini et al. [8]. A similar method has proved effective on the Siemens Inveon detector by Hu et al. [9]. The method can achieve high accuracy for their specific detectors, but suffers from instability due to inconsistencies in training data. A crystal identification method using non-rigid registration to a Fourier-based template was proposed by Chaudhari et al. [10]. The method has a good effect on crystal identification, but it is time-consuming to generate a template image non-automatically. What is more, the edge searching based algorithm and principal component analysis based algorithm were also proposed to build a crystal position lookup table [11, 12].

In this work, a new general method is presented for building a crystal position lookup table based on the region segmentation algorithm. This approach is especially pertinent for the position histogram, having a large dimension and non-uniform intensity distribution, and a high robustness in the position histogram with irregular spots position distribution.

2 Methods and materials

In this algorithm, each crystal marking point corresponding to a single crystal must be identified in the position histogram first. Then, crystal boundary points are determined by finding the centers of every four local neighboring crystal marking points. The position histogram is segmented into regions by connecting the adjacent crystal boundary points [7]. Each region is labeled by the corresponding crystal index, which is the crystal position lookup table. The processing flow is shown in Fig. 1.

In the whole process, the key procedure is to identify crystal marking points accurately. Several image processing methods are used to reduce noise and enhance the contrast in the position histogram image. Then the position histogram is divided into many disconnected regions by threshold segmentation. After that the centroid of each region is chosen as the corresponding crystal

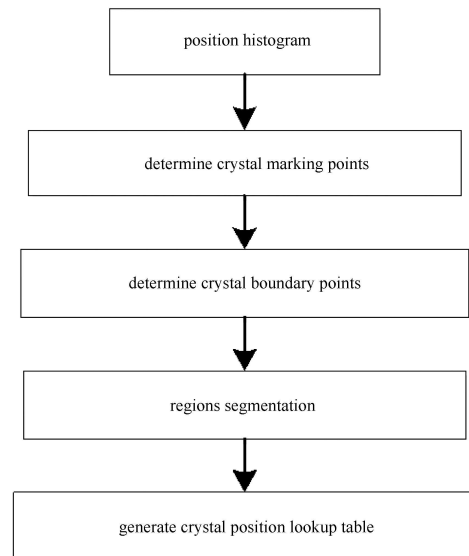


Fig. 1. Processing flow for generating crystal position lookup table using a position histogram.

marking point. The processing steps are depicted in detail as follows.

2.1 Noise reduction

The position histogram acquired from the detector includes much noise, which may give rise to mistaken segmentation. A mean filter with a 3×3 kernel is applied to minimize the noise. A larger kernel results in greater noise reduction, but also causes serious degradation of normal spots. In addition, the background is cleared in order to reduce the noise and accelerate the following procedures. Generally, an approximate average intensity of the position histogram is chosen as the background threshold. The pixels that are less than the threshold are removed, and only the remaining pixels are processed by the following steps. The selection of the threshold depends on the signal to noise ratio and non-uniformity of the position histogram. However, it has a small effect on the result.

2.2 Normalization

Due to the difference in detection efficiency in the detector module, the distribution of spots intensity is non-uniform in the position histogram. It is hard to choose a uniform threshold for image segmentation. The normalization procedure is to make each local region have a similar intensity. After clearing the background, the position histogram has been divided into several disconnected regions. The average intensity of each region is denoted by A_{l_i} , and i is the index of the region. The global average intensity of all regions is A_g . The normalization factor of A_g/A_{l_i} is multiplied by each pixel of the i -th region, which can adjust the position histogram to a uniform level of intensity.

2.3 Histogram equalization

Histogram equalization can increase the contrast of the position histogram by spreading out the frequent intensity values [13], and make the spots have a similar size and intensity. This process is beneficial to the following threshold segmentation procedure. First, the position histogram is scaled to a certain range, L , linearly. Then let N_k be the number of pixels with intensity k , and k has a range from 0 to $L-1$. The total pixels are denoted as

$$N = \sum_{k=0}^{L-1} N_k. \quad (1)$$

Then the new pixel intensities are obtained by transforming the pixel intensities, k , by the function

$$T(k) = \text{floor} \left(L \sum_{i=0}^k \frac{N_i}{N} \right). \quad (2)$$

Where $\text{floor}()$ rounds down to the nearest integer.

2.4 Threshold segmentation

Through a series of processing methods, the position histogram has a better distribution, and all the spots have a similar shape and characteristic. The next procedure is to find an appropriate threshold to segment the position histogram. The principle of selecting the threshold is that the number of isolated regions segmented is as close as possible to the crystals number.

2.5 Find crystal marking points

The centroid of each segmented region is picked as the crystal marking point. The average of all the pixel coordinates of the region is calculated to determine the position of the central pixel. However, it is not certain that all the crystal marking points are identified accurately. It is more likely to miss some regions using the higher segmentation threshold, or merge some regions when a relative lower threshold is selected. So interactive correction is carried out, which will make sure that all the crystal marking points are identified accurately. The interactive correction is implemented by clicking the mouse in the graphical user interface (GUI) of the software system, which can remove the mistaken marking points and add the missing marking points. In addition, the system can give the prompt message of approximate locations needing correction interactively, which is based on the relative position and intensity of each neighboring marking points.

2.6 Generate crystal position lookup table

When all the crystal marking points are found, the crystal boundary points, that are also called valley points, can be determined by calculating the centroid

position of each four neighboring crystal marking points. Then the position histogram is divided into a grid by connecting the adjacent crystal boundary points. Each mesh region corresponds to a crystal element. The crystal position lookup table is built by filling each region with the corresponding crystal index.

3 Result

The algorithm was implemented in C programming language, and integrated in the quality control module of the PETCTview software system developed by the Institute of High Energy Physics, Chinese Academy of Sciences. The GUI, shown in Fig. 2, was designed and implemented in Qt, which can guide us to complete all the procedures conveniently. The GUI also provides the function of acquiring the position histogram, displaying the image, correcting crystal marking points interactively, and uploading the crystal position lookup table to the device. What is more, the algorithm was verified in the breast dedicated single photon emission tomography system (SPEMi) which was also developed by the Institute of High Energy Physics, Chinese Academy of Sciences.

3.1 Building crystal position lookup tables in a whole-body PET detector

For the whole-body PET scanner, there are 256 detector blocks in total, and each block consists of an 11×11 array of LYSO crystals coupled with H8500 PMT. Each crystal element has the size of $3.5 \text{ mm} \times 3.5 \text{ mm} \times 25 \text{ mm}$. The position histograms are obtained using Ge-68 rod source revolving around the scanner ring, and have a resolution of 128×128 pixels. The position histogram of the detector block 0 is shown in Fig. 3, which indicates that 11×11 spots are distinguished clearly.

The processing and segmentation results of the position histogram are presented in Fig. 4(a)–(d). Brighter

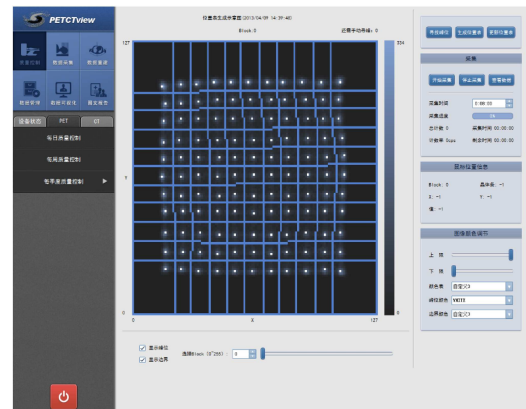


Fig. 2. GUI for building the crystal position lookup table implemented in the quality control module of the PETCTview software system.

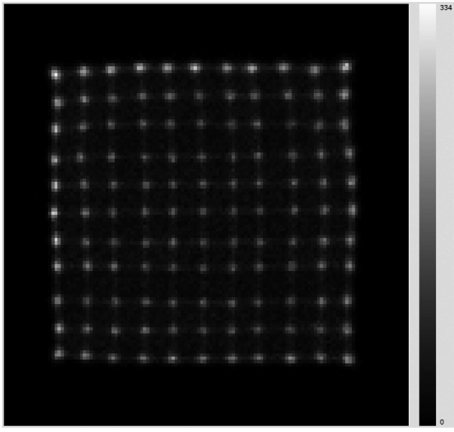


Fig. 3. A position histogram image using the Ge-68 rod source acquired in the whole-body PET detector.

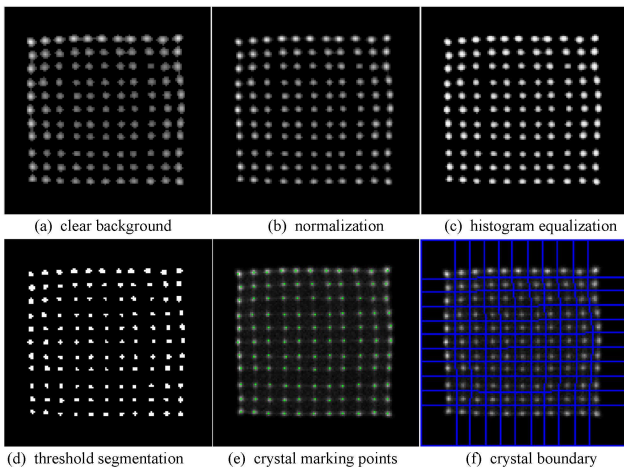


Fig. 4. Processing results using the region segmentation based algorithm in a whole-body PET detector.

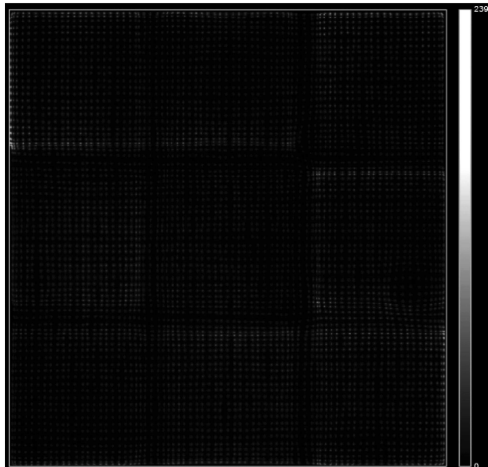


Fig. 5. A raw position histogram image of the Tc-99m flood source acquired in a SPEMi detector.

pixels represent higher intensity levels. The result of finding crystal marking points is shown in Fig. 4(e), and

the green points represent the crystal marking points. The result of building crystal boundaries is shown in Fig. 4(f), and the blue lines represent the crystal boundaries.

3.2 Building crystal position lookup table in a SPEMi detector

The SPEMi detector module consists of a NaI crystals array and nine H8500 PMTs array. The crystals array is of a 77×77 matrix with the element size $1.8 \text{ mm} \times 1.8 \text{ mm} \times 6 \text{ mm}$. The position histogram measured by the SPEMi detector using Tc-99m flood source is shown in Fig. 5, which has a resolution of 1024×1024 pixels. The result indicates that only 75×75 spots are distinguished, which is due to the adjacent rows and columns merging together in the borders of the position histogram.

The processing and segmentation results of the position histogram are presented in Fig. 6(a)–(d). The result of finding crystal marking points is shown in Fig. 6(e). The result of building crystal boundaries is shown in Fig. 6(f).

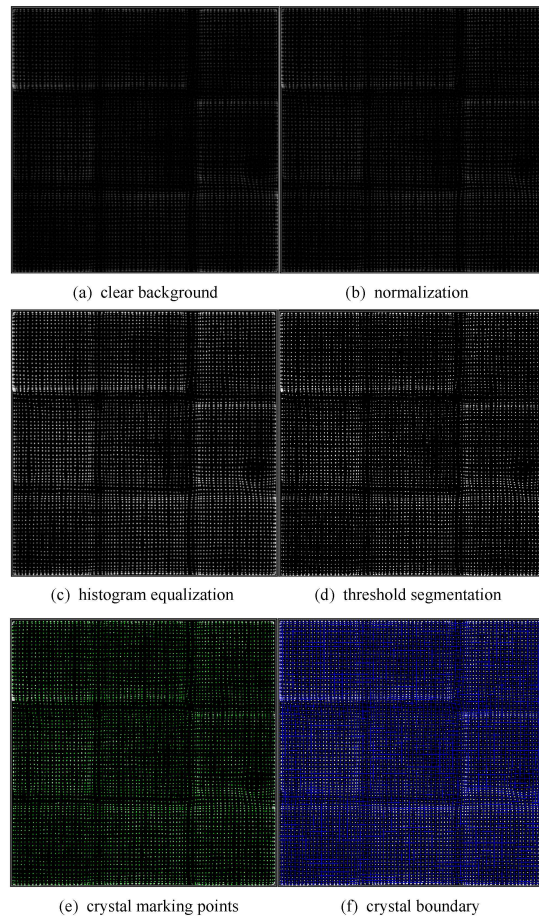


Fig. 6. Processing results using region segmentation based algorithm in a SPEMi detector.

4 Discussion

The approach to building the crystal position lookup table can broadly be divided into three processes. (i) Segment the position histogram into disconnected regions. (ii) Determine the crystal marking points. (iii) Determine the crystal boundaries. The segmentation process is the most critical, which will directly affect the efficiency of building the crystal position lookup table. The accurate crystals identification will decrease the consuming time of the interactive correction, so the percentage of the identification of the crystal marking points is as the evaluation of the algorithm.

To the position histograms of whole-body PET detectors, all the crystal marking points in 256 detector blocks have been identified accurately, and the interactive correction procedure can be skipped. It takes no

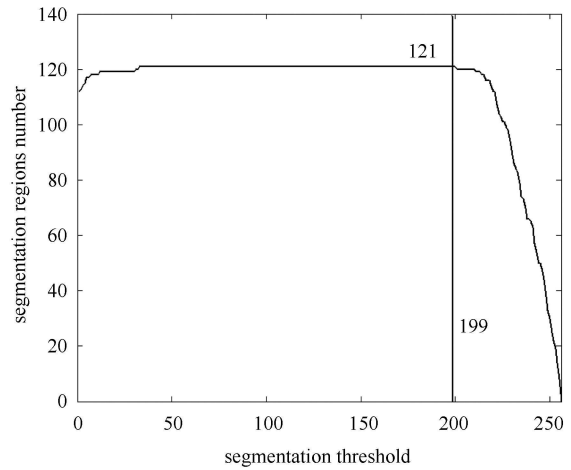
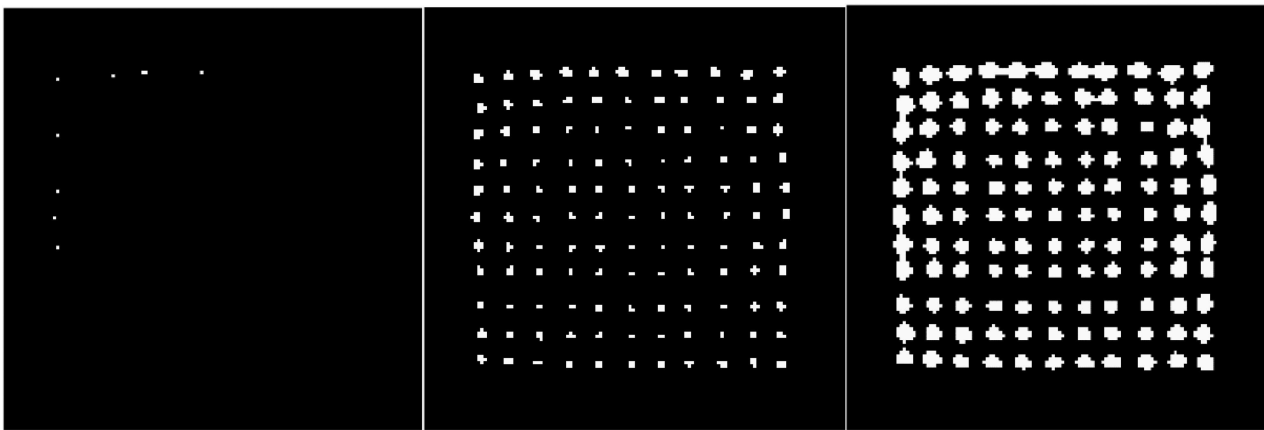


Fig. 7. Region number of segmentation changing with different thresholds in detector block 0 of PET.



(a) threshold=255 (b) threshold=199 (c) threshold=0

Fig. 8. Segmentation results with different thresholds in detector block 0 of PET.

more than 2 seconds to build the $11 \times 11 \times 256$ crystals position lookup table in Intel(R) Core(TM) i5-2400 3.10 GHz CPU.

Among the distinguishable 75×75 spots of the SPEMi position histogram, 99.23% crystal marking points are identified accurately, and only 59 crystal marking points, including 16 mistaken location points and 43 missing location points, need to be corrected interactively by clicking the mouse. The mistaken and missing marking points appear primarily in the borders due to the merging of two adjacent spots, and in the joint parts of PMTs due to the dead gaps. These regions of the position histogram have bad distribution characteristics.

For different characteristic position histograms, it is necessary to adjust the segmentation threshold subtly to get a better segmentation effect. That will shorten the interactive correction time and increase efficiency.

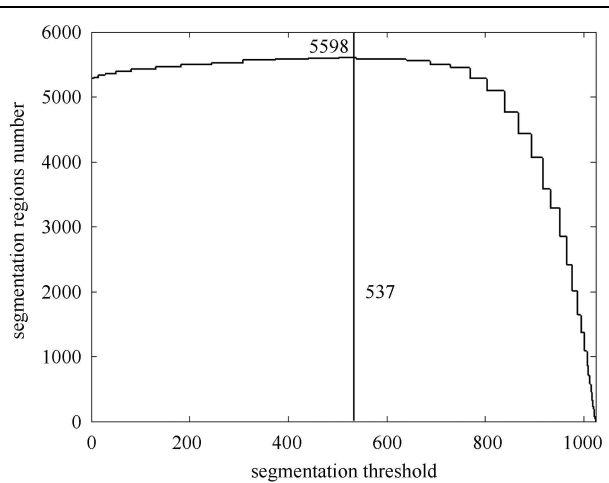


Fig. 9. Region number of segmentation changing with different thresholds in a SPEMi detector.

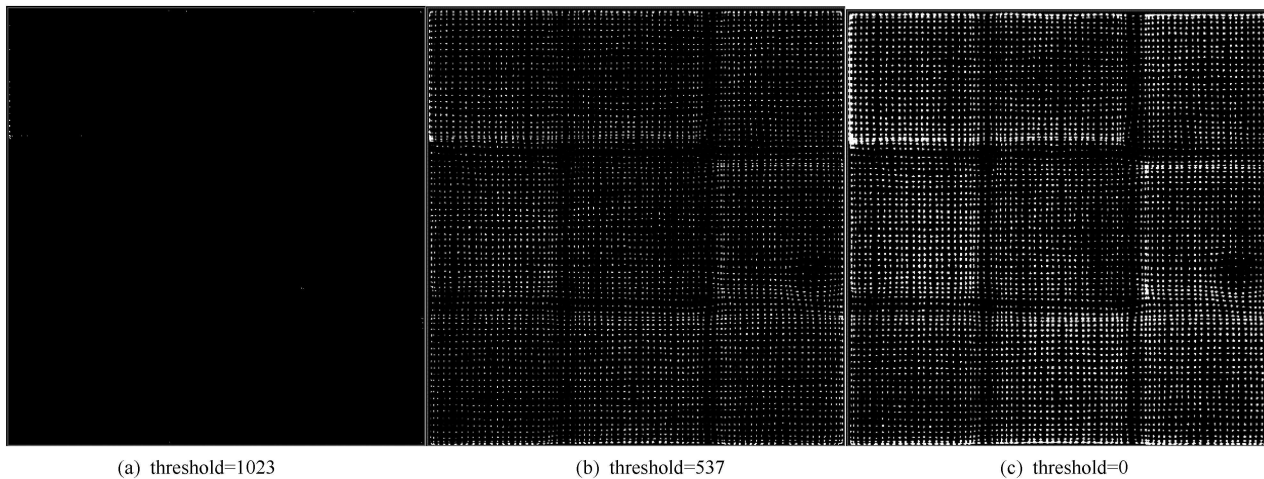


Fig. 10. Segmentation results with different thresholds in a SPEMi detector.

Generally, the relative high threshold generates small segmentation regions. The small regions have a high proportion of true events, and can reduce the noise effect. In this work, many trials are performed with the threshold changing in descending order among a certain range, and the number of segmentation regions goes up first, and then declines with the decreasing threshold. The first threshold of closest total crystals number is picked as the final segmentation threshold.

In the position histogram of whole-body PET detectors, the intensity levels are scaled from 0 to 255. The selection of the scaling range depends on the quality of the position histogram. In general, a large scaling range needs to be chosen when the position histogram has a bad distribution characteristic. The region number of segmentation changing with different thresholds in detector block 0 is shown in Fig. 7. The 199 is chosen as the final segmentation threshold. The results of segmentation with different thresholds are shown in Fig. 8. As to the SPEMi detector, the intensity levels are scaled

from 0 to 1023. Similar results are shown in Fig. 9 and Fig. 10, and the 537 is chosen as the final segmentation threshold.

5 Conclusion

In this paper, a region segmentation method has been presented for building a crystal position lookup table in a scintillation detector. Since the method does not rely on specific characteristics of detectors, it can be adapted to work with all kinds of scintillation scanners and any configurations of crystal arrays. It was proved to be highly accurate, efficient and robust in the whole-body PET detector and SPEMi detector developed by the Institute of High Energy Physics, Chinese Academy of Sciences. Moreover, the method is effective in a variety of position histograms, and has an advantage in the position histogram with a large dimension, non-uniform intensity distribution or a high degree of distortion.

References

- 1 John L H, Anatoly R, Alberto D G. *Eur. J. Nucl. Med. Mol. Imaging*, 2003, **30**(11): 1574
- 2 Juan J V, Jurgen S, Stefan S et al. *IEEE TRANSACTIONS ON MEDICAL IMAGING*, 1998, **17**(6): 967
- 3 Anger H O. *Journal of Nuclear Medicine*, 1964, **5**: 515
- 4 Cutler P D, Hoffman E J. *IEEE TRANSACTIONS ON MEDICAL IMAGING*, 1994, **13**(2): 408
- 5 John W Y, Moyers J C, Mark L. *IEEE TRANSACTIONS ON NUCLEAR SCIENCE*, 2000, **47**(4): 1676
- 6 Kelly A S, Michael T J. *IEEE TRANSACTIONS ON NUCLEAR SCIENCE*, 2004, **51**(1): 85
- 7 CHAI Pei, SHAN Bao-Ci. *Science in China Series E: Technological Sciences*, 2008, **52**(8): 2418
- 8 Lazzarini B, Marcelloni F, Marola G. *Electronics Letters*, 2004, **40**(6): 360
- 9 HU Dong-Ming, Timothy G. *Nuclear Science Symposium Conference Record*, 2007. M13-13: 2847
- 10 Abhijit J C, Anand A J, Spencer L B et al. *Phys. Med. Biol.*, 2008, **53**(18): 5011
- 11 Kun Di. *Edge-Based Peak Position Search Algorithm for PET Detectors*. 2011. California State University, Sacramento
- 12 Johannes B, Klaus W. *IEEE TRANSACTIONS ON NUCLEAR SCIENCE*, 2009, **56**(3): 602
- 13 Rafael C G, Richard E W. *Digital Image Processing*. Second Edition. Publishing House of Electronics Industry, 2003. 72